communications materials

Article

https://doi.org/10.1038/s43246-024-00680-4

Multi-sensing yarns for continuous wireless sweat lactate monitoring

Bradley Napier[1], Giusy Matzeu[1] & Fiorenzo G. Omenetto[1,2]

Textile integrated sensors based on conductive, electrochemically active microfibers can enable inexpensive, nearly invisible distributed sensing of sweat in clothing. Reduced graphene oxide fibers are mechanically robust, conductive, and can be easily functionalized to form a variety of sensors with properties comparable to planar fabricated sensors, given their ability to work both as electrical interconnections and as a base electrode. Here, we present an electrochemical yarn based on modified dry-spun reduced graphene oxide fibers. This braided format contains reference, counter electrode, a lactate-responsive fiber functionalized with lactate oxidase, and a pH-sensing fiber for calibration in a single, robust, weavable format. This electrochemical yarn was integrated into a demonstrator wearable textile-patch capable of continuous data collection and wireless data transmitted to an ad-hoc app. The yarns perform comparably to traditional probes in a format of broad utility for standalone or integrated monitoring of physiological parameters.

Sensors for measuring biomarkers in eccrine sweat have progressed rapidly with multiple demonstrations of flexible, stretchable planar devices and tattoo format sensing units over the past decade[1–8]. These sensors have enabled real-time monitoring of hydration, athletic performance, and stress with in situ and non-invasive measurements of salts, metabolic products, and other biomarkers[9,10]. Recent efforts have aimed at further integrating these sensors into 1-D weavable textile materials[11–13]. Doing so would enable invisible sensor fibers that could be envisioned as a grid of sensing filaments embedded throughout a textile, spanning larger areas for more detailed physiological understanding. Textile-based sensors utilizing novel nanomaterials and functionalization approaches are uniquely capable of meeting this goal, providing strong, electrochemically stable, and tunable materials that operate as both electrode and weavable electrical interconnects[14].

There are few flexible fibers that meet the requirements needed for an electrochemical textile electrode. CNT fibers/yarns, nanowire elastomeric fibers, carbon-coated threads, and reduced graphene oxide (rGO) fibers are some of the candidates for this purpose[11–15]. Fibers have also recently been produced from other 2D materials, such as MXenes, with excellent electrical and electrochemical properties[16]. rGO fibers are the most economically viable option as they can be produced using graphite flake—an inexpensive bulk material either from natural sources, or synthesized at low cost[17,18]. These polymer-free fibers are self-assembled from monolayer graphene oxide (GO) flakes, then reduced, forming tough, conductive fibers held together by Van der Waals forces[15]. While short segments of rGO fibers have been used as temperature sensors, gas sensors, and benchtop hydrogen peroxide (H_2O_2) sensors, they have yet to be applied to wearable enzymatic sensors[19–22].

With controllable diameters on the microscale, excellent electrochemical (−0.9 V to 1 V electrochemical window, as high as 10^6 S m^{-1} conductivity) and mechanical properties (as high as $\varepsilon > 300$ GPa, UTS > 3 GPa), pure rGO fibers are an excellent base material as they can be tailored to suit the application's needs with a multitude of functionalization possibilities[23,24]. Given the abundance of functional groups in graphene (e.g., epoxy, hydroxyl, carboxyl), the surface can be tailored to the application, increasing capacitance by adding redox groups (e.g., ferrocene), altering mechanical or electrical properties, or adding specific functional groups to enhance post-process modifications[17,25–27]. The fibers can also be doped with various nanomaterials from 0D to 2D such as MXenes, cellulose nanocrystals, metallic nanoparticles, increasing strength or altering electrical properties[22,28–31]. Additionally, the reduced fibers can also be functionalized in the same way as rGO, with either electro- or electroless deposition of nanomaterials and/or conducting polymers[11,32]. Dip coating and spray coating enable chemically selective electrodes, reference electrodes, and insulating coatings[11,12]. Combining various functionalization approaches enables numerous textile-integrated applications in biochemical and bioelectrical sensing as well as photovoltaics and supercapacitors[32].

For enzymatic sensors, rGO has been used as the base electrode or with additives such as metal catalyst nanostructures, redox moieties, and Prussian Blue (PB) among others for improved performance[33]. Functionalization with these materials allows for either indirect measurement of enzyme activity through H_2O_2 (e.g., mediated by platinum, PB) or direct

[1]Silklab, Department of Biomedical Engineering, Tufts University, Medford, MA, USA. [2]Department of Electrical and Computer Engineering, Tufts University, Medford, MA, USA. e-mail: fiorenzo.omenetto@tufts.edu

measurement through redox mediators (e.g., tetrathiafulvalene (TTF)) at lower operating potentials[1,5,6,8].

As a low-cost sensor platform, bundles of these fibers can enable the fabrication of electrochemical yarns useful for both textile-integrated sensing applications (sweat, gas, viral/microbial) as well as a potential low-waste disposable sensor alternative to screen printed carbon electrodes[32]. Screen printing generates a lot of non-recyclable waste and uses harsh chemicals, making it less sustainable than the proposed fibers.

In this work, rGO yarns were developed for wearable sweat sensing. Functionalized with platinum nanoparticles (Pt NPs) and a biopolymer membrane for lactate sensing, these small form factor (~100 μm diameter) multiplexed sensor yarns are constituted by bundling a reference, counter electrode, and pH sensing fibers in a single convenient format.

Sweat contains a variety of salts, metabolic products, and other biomarkers indicative either of overall health or current state (fatigue, stress)[9]. Often measured is L-lactate, the metabolic product produced at increasing rates with muscle fatigue. This is typically measured with colorimetric or electrochemical sensors using lactate oxidase (LOx). Although specific to L-lactate, these sensors have various redox and reactive species (e.g., ascorbic acid, uric acid) whose interference can be avoided using selectively permeable membranes underneath the enzymatic layer (e.g., p-Phenylenediamine, Nafion)[34–36]. Other parameters, such as temperature and pH, can be measured simultaneously to allow for error correction in the sensor's current output[1]. This is because enzymes are strongly dependent on these factors. Reaction rates increase exponentially with temperature, up to 50 °C, beyond which irreversible thermal denaturation of the protein occurs for most enzymes. The enzyme's working pH range varies depending on the enzyme itself, the matrix, and the temperature, so pH must be considered when detecting the analyte (i.e., lactate in this specific case)[37].

Results and discussion

Fiber preparation

rGO fibers were fabricated based on dry-spinning from liquid crystal GO. GO was produced via an improved Hummers' method from natural graphite flake (+100 mesh), producing GO sheets with an average lateral size of 30 μm. GO fibers were dry-spun (100–200 μm needles), then reduced in ethanolic hydriodic acid, producing fibers with strong mechanical properties ($\varepsilon > 6$ GPa, UTS > 200 MPa, >9% breaking elongation), and high conductivity (18 kS m^{-1})[27]. Further improvements to the mechanical and electrical properties can be achieved through control of sheet dimensions, drawing, and post-processing the chemically reduced fibers with joule heating, as established in the literature[24,38–40]. Based on material cost at lab scale, these fibers are also economical, with cost estimated to be ~$0.03 per meter.

The multi-sensor electrochemical yarn was then developed based on the rGO fibers described above by combining 4-fibers: a three-fiber lactate sensor (i.e., reference, counter, and working electrode fibers) with a pH ion-selective electrode (ISE) fiber, leveraging the same reference fiber used for the lactate sensing unit. These fibers can be braided together to form a yarn that can subsequently be connected to an integrated circuit for signal processing and wireless readout (Fig. 1 and Fig. S4). The fabrication and operation of the pH and reference electrode fibers were described previously[27]. The counter electrode and lactate sensor are based on platinum nanoparticle-impregnated rGO fibers with the latter also coated with a biopolymer enzymatic layer, both described below.

Preparation/characterization of PtNP-rGO

Platinum nanoparticles were deposited on rGO fibers using a one-pot polyol synthesis process, which has been extensively used for fabricating various metallic nanoparticles supported on carbonaceous materials (rGO, carbon black, and CNTs)[41–46]. In this process, hexachloroplatinic acid is reduced by ethylene glycol. The pH of the reaction is adjusted with NaOH (4:1 molar ratio NaOH:Pt) in order to generate uniform nanoparticles[47]. During the reaction, the pH of the reaction drops and a large zeta potential difference (> 30 mV) between the fiber and nanoparticles allows for efficient particle binding, forming PtNP-rGO[41,42]. Prior to functionalization, the rGO fibers were plasma treated, increasing the surface energy, porosity, and adding surface functional groups—all improving nanoparticle adsorption[48,49]. Alternatively, grafting functional groups to rGO prior to spinning or platinization may also improve binding and dispersion efficiency as has been demonstrated with rGO and CNTs, albeit with more processing steps[50,51].

A spool of PtNP-rGO is shown in Fig. 2A, while scanning electron microscopy (SEM) images of the fiber (35 μm diameter) post-functionalization show a uniform coating of small particles with larger visible aggregates (Fig. 2B). Refer to Fig. S9 for the schematic that summarizes the PtNP-rGO fiber preparation.

To confirm platinization of the rGO fibers, 15 mm segments of fiber were analyzed via cyclic voltammetry (CV) in 0.5 M sulfuric acid (Fig. 2C). Broad hydrogen adsorption/desorption peaks are visible between −350 and 0 mV. Nanoparticle adsorption on the fiber was quantified from the total hydrogen desorption charge using the equation[52]:

$$ESCA = \frac{Q_H}{\theta * Q_{ML}} \quad (1)$$

where Q_H is the integrated charge from H^+ desorption, θ is the surface coverage of H^+ (assumed $1H^+$ per Pt surface center), and Q_{ML} is the normalized charge needed to desorb a monolayer of H^+ (210 μC cm^{-2}, assumed

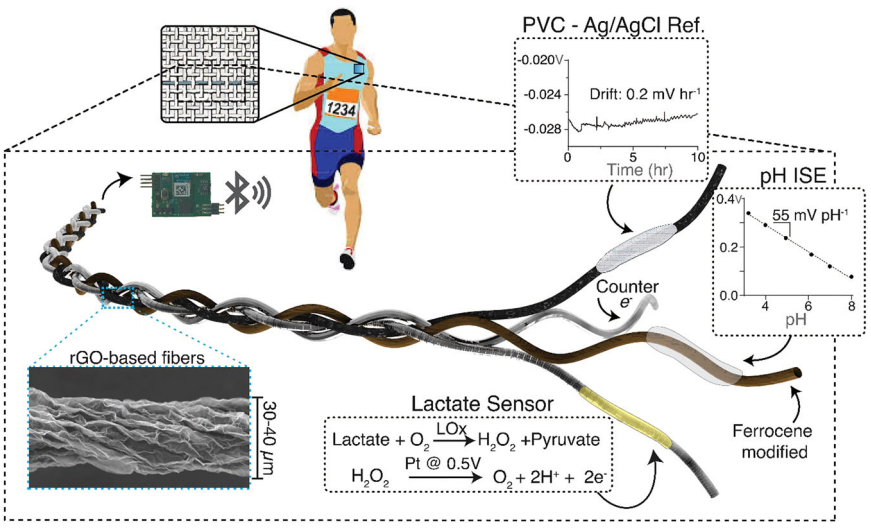

Fig. 1 | Overview of braided rGO-fiber sensor platform. The multi-sensing lactate braid consists of 4 fibers—3 fibers for the lactate sensor, 1 for pH calibration. The lactate sensor fibers are built as follows: one rGO fiber with spray-coated reference membrane, a platinized rGO fiber as a counter electrode, and a platinized rGO fiber coated with the enzymatic membrane for lactate detection. The pH sensor is a spray-coated polymeric ISE membrane on a ferrocene functionalized rGO transducer fiber.

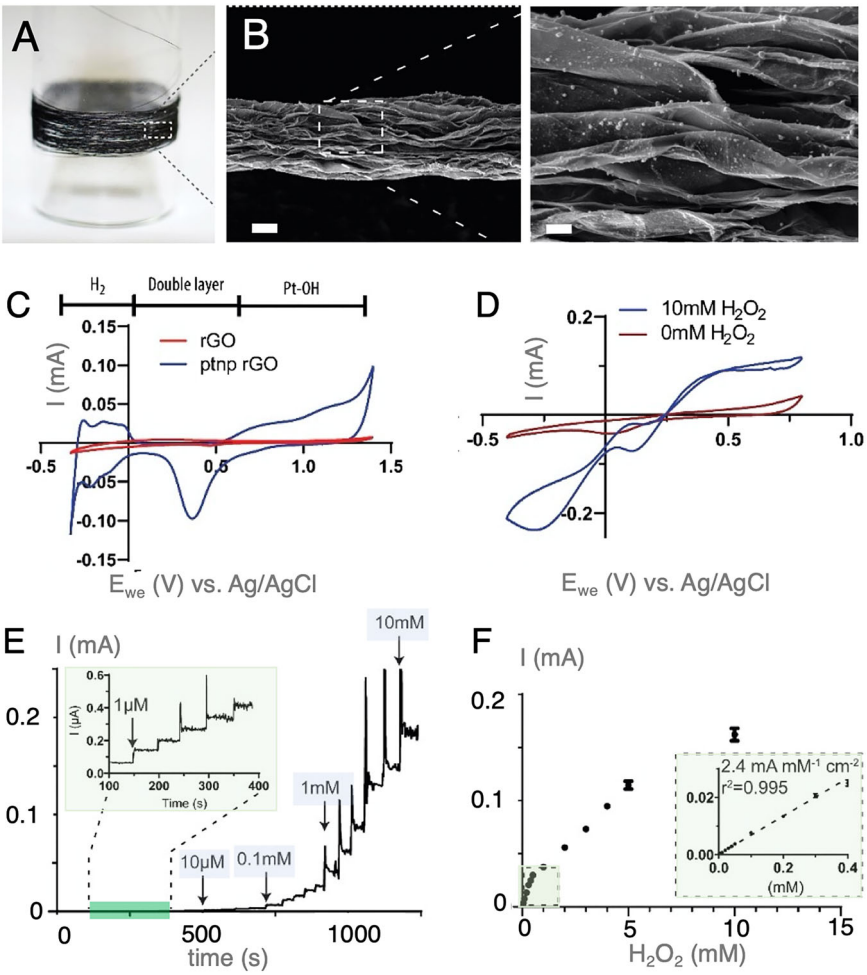

Fig. 2 | Fiber electrochemical characterization and performance. A Spool of PtNP- rGO fiber. **B** SEM of PtNP-rGO fiber (scale bar = 10 μm) and magnified inset (scale bar 2 μm). **C** CV of rGO and PtNP-rGO in 0.5 M H_2SO_4. **D** CV of PtNP-rGO in 100 mM NaCl before and after addition of 10 mM H_2O_2. **E** Chronoamperogram of PtNP-rGO with successive additions of H_2O_2 (5 steps of 1 μM, 10 μM, 0.1 mM, 1 mM, with half increments between steps). Concentration noted at each order of magnitude. Inset shows first additions starting at 1 μM. **F** Calibration curve extracted from chronoamperograms (3 replicates). Inset shows low concentration region, with linear fit of 67.8 μA mM^{-1} or 2.4 mA mM^{-1} cm^{-2} when normalized to geometric surface area. All PtNP-rGO fibers were cut to length having dimensions of: l = 15 mm, d = 30–35 μm.

equal proportion of 100,111,110 planes). The estimated surface area is 0.45 cm^2 per cm length of fiber or ~23.7 times the geometric surface area. PtNP-rGO fibers also exhibit a large decrease in impedance compared to bare rGO fibers as shown from electrochemical impedance spectroscopy (EIS) measurement (Fig. S2). Maximal loading was experimentally determined to be 10 mM $PtCl_6^{-2}$ with 40 mM NaOH. Further increases of Pt were found to inhibit nanoparticle formation, while lower NaOH quantities produced large aggregates, poor loading efficiencies, and inferior stability for H_2O_2 sensing.

The biosensor detects H_2O_2, a byproduct of the enzymatic reaction between LOx in the sensing membrane and lactate in the surrounding solution. LOx converts lactate to pyruvate using oxygen (Fig. 1). Lactate concentrations can be easily correlated to the initial lactate concentration in the biosensor's surroundings, and more importantly, the oxidation of lactate will produce a current that is specific to the target analyte.

Therefore, the sensitivity of the PtNP-rGO fibers was measured with CV and chronoamperometry (CA) at 0.5 V vs Ag/AgCl (Fig. 2D–F). In 10 mM H_2O_2, onset of catalytic current is evident above 0.3 V, with saturation near 0.5 V, thus measurement can be performed at lower bias (e.g., 0.4 V) with a small decrease in sensitivity if desired (Fig. 2D). Bubble formation causes noise in measurements evident in both CV and CA measurements at higher concentrations. PtNP-rGO has a limit of detection (LOD) of 0.2 μM for H_2O_2, with a clear increase in current for every additional 1 μM of H_2O_2 (Fig. 2E). The sensor shows two linear ranges, the first encompassing three orders of magnitude from 0.2 μM to 400 μM of H_2O_2, the second from 0.5 μM to 5 mM of H_2O_2. The fiber exhibits a high sensitivity of 67.8 ± 0.3 μA mM^{-1}, or 2.4 mA mM^{-1} cm^{-2} when normalized to the surface area for the first linear range. The high sensitivity can be attributed to the large surface area of dispersed platinum nanoparticles and wrinkled nature of the rGO surface. Additionally, the PtNP-rGO fiber exhibits high stability with 93.5% of current retained after 14 h of continuous polarization in 1 mM H_2O_2 without additional coatings (Fig. S1A).

The best-conducting substrates for lactate sensors reported in the literature are CNT/TTF complexes (sensitivity of 4.8 μA mM^{-1}, linear range up to 24 mM, stability of 97% after 1 h, and unspecified LOD)[8,53,54]. These sensors also have a low operating potential (<0.2 V vs Ag/AgCl), which prevents interference from easily oxidized species (e.g., ascorbic acid and uric acid). However, these electrodes are developed in a flat format, with either buckypaper soaked with TTF solution or CNT dispersions sonicated with TTF, then drop-cast to form thick coatings. The CNT matrix slows the leakage of the soluble, oxidized TTF^+ from the sensor, while allowing for infiltration of the enzymatic coating. Coating rGO fibers with these dispersions may produce sensors with poor sensitivity and stability because of the lack of porosity of conductive supports of this kind (e.g., CNT matrix, carbonaceous fibers). This approach is also difficult to implement in a fiber format, as it may decrease the sensor's flexibility.

Platinum was the original electrode of choice for enzymatic sensors, but its high cost, potential fouling with proteins, and higher applied potential (> 0.4 V) have made it less popular for these applications. However, the high surface area of platinum nanoparticles reduces the amount of material used and thus the cost. For lactate sensors, the requirement of a diffusion-limiting layer and thick enzymatic membranes decreases the risk of biofouling, and potentials of 0.5 V do not have noticeable interference from common sweat interferants (see the "Lactate sensor preparation/characterization" section for more details).

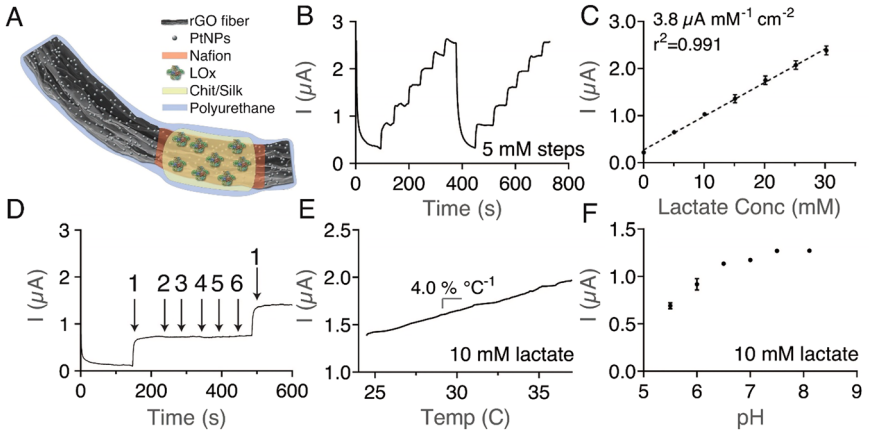

Fig. 3 | Sensor performance. **A** Diagram depicting elements of lactate sensor fiber. **B** Chronoamperogram of lactate sensor. **C** Calibration curve extracted from chronoamperograms (3 replicates). **D** Interference test of lactate sensor in 10 mM phosphate buffer (pH 7.4). 1: 5 mM lactate, 2: 10 mM Na^+, 3: 1 mM Ca^{2+}, 4: 1 mM Mg^{2+}, 5: 1 mM glucose, 6: 100 μM ascorbic acid. **E** Temperature response of lactate sensor in 10 mM phosphate buffer and 10 mM lactate. **F** pH response of lactate sensor in 10 mM phosphate/citrate buffer with 10 mM lactate (3 replicates). All lactate sensors had coated lengths of 15 mm.

Solution-based deposition allows for evenly coating large lengths of fibers at a time, enabling rapid sensor fabrication. As compared to electrochemical depositions, this method has increased uniformity along the length of the fiber (gradient deposition due to the resistive fiber) and scalability (spool vs. individual segments).

Lactate sensor preparation/characterization

For the realization of enzymatic membranes and their characterization, lactate sensors were fabricated on PtNP-rGO fibers using a multi-layer approach common to platinum-oxidase enzyme systems (Fig. 3A)[6]. The membranes and coating methods are tailored to increase the linear range of the sensors to cover relevant physiological values, namely using ranges of lactate concentration in sweat between 5 and 30 mM, as the Michaelis-Menten constant (K_m) for LOx (Toboyo) is 1 mM[36,55].

First, fibers were coated with a permselective Nafion membrane as an interference rejection layer. Next, the fibers were dip-coated in the active layer containing LOx embedded in a biopolymer matrix consisting of LOx, chitosan, and silk fibroin. To increase the linear range, the enzymatic layer needs to be thicker than for other sensing systems, such as glucose[1]. Pre-crosslinking the biopolymer matrix with a low concentration of glutaraldehyde increases the viscosity of the mixture allowing for deposition of a thick layer (~5–10 μm thick) on the fiber in a dip-coating process. Without the pre-crosslinking step, a thinner coating exhibiting higher sensitivity, but decreased linear range (<5 mM) was observed. Finally, the membrane was spray-coated with a layer of polyurethane (PU), acting as a diffusion-limiting layer to further extend the linear range of the sensor into the clinical range for sweat[56]. Spray-coating was found to improve both speed of fabrication and repeatability of the diffusion layer as multiple dip coatings produced variable thicknesses based on redissolution of the previous layer. It was found that spray coating with 0.25% PU in THF could produce sensors with a linear range up to 30 mM, depending on the applied thickness. Higher concentrations (1% PU) produced nonuniform coatings and linear ranges limited to 15 mM with similar maximum output current per length (I_{max} ~ 2 μA cm^{-1}). SEMs of the PU-coated enzymatic membranes from both 1% and 0.25% are shown in Fig. S3.

Fabricated sensors (15 mm lengths) were characterized for sensitivity and various interferences to lactate. The output of the sensor in response to a sequential series of 5 mM increments of lactate is shown in Fig. 3B, with corresponding calibration curve shown in Fig. 3C ($n = 3$): LOD of 0.7 mM ($3\sigma_{bl}$/m), sensitivity of 3.8 μA mM^{-1} cm^{-2}, and a relative standard deviation of 4.5%. Additions of various cations (10 mM Na^+, 1 mM Mg^{2+}, 1 mM Ca^{2+}) as well as glucose and 100 μM ascorbic acid (simulating the interferants commonly found in sweat) had negligible effect on the output current of the sensor (Fig. 3D). The sensors showed high operational stability, retaining 97% of initial current after more than 2 h of continuous polarization in 20 mM lactate (Fig. S1B).

As expected for enzymatic sensors, pH and temperature have larger impacts on the sensor response. With change in temperature measured in 10 mM lactate, the output current is linearly correlated with a slope of 4.0% C^{-1} in the range of 24–37 °C (Fig. 3E). Larger changes are observed for pH; at pH 5.5, the sensor has an output of 54% compared to the maximum output recorded in the range pH 7–8 (when measured in 10 mM lactate) (Fig. 3F). As pH in sweat can vary both during exercise and between people or measurement location on the body, it is necessary to concurrently monitor pH alongside the lactate sensor output. In order to account for this, a pH sensor fiber is included in the yarn configuration in order to allow for continuous calibration during sensor use. Biosensors are most sensitive at the optimal pH and temperature, but they can still be accurate even if operating outside of these conditions, as long as the pH and temperature dependencies are accounted for.

Preparation and use of sensing yarn-based demonstrator device

As a demonstration of the sensor platform using the fibers described previously, a yarn consisting of a four-fiber braid is fabricated combining a three-electrode lactate fiber sensor and a pH ion selective (ISE) fiber sensor using a shared reference electrode. The lactate sensor is composed of the PtNP-rGO fiber counter electrode, and an rGO fiber-based reference electrode. The reference electrode membrane is a fiber spray-coated with heterogenous PVC-Ag/AgCl-KCl layer, exhibiting low drift (0.2 mV h^{-1}) in artificial sweat with minimal sensitivity to solution composition[27,57]. The pH sensor is fabricated by spray-coating a polymeric ISE membrane on a ferrocene-modified rGO fiber for enhanced capacitance/stability (55.8 mV pH^{-1}, Fig. S5)[27]. (Additional fabrication methods for the pH sensor and reference electrode are provided in Supplementary Information). The fibers are then interfaced to a socket connector and braided up to the active region (which spans 10 cm in length in each of the fibers) to form the sensor yarn. (Additional details on the yarn assembly and braiding are described in ref. 27).

The sensing yarn is subsequently integrated into a wearable patch (Fig. 4A, C) as a demonstrator device. First, the yarn is woven into a rectangle of adsorbent linen fabric and subsequently encapsulating the sensing area between patterned gauze and filter paper, which is then sealed with patterned PET (FLEXcon) with double-sided adhesive. When adhered to the skin, sweat is channeled through the gauze, then wicked through the filter paper. The wicking of the patch allows for improved temporal measurements in comparison to either direct skin contact or to the use of a single piece of absorbent material (Fig. S8). Options are also available for direct integration with microfluidic thread structures, or into more sophisticated microfluidic skin patches[58,59].

A custom interface to the sensing yarn is built by combining a Bluetooth-based wireless readout circuit (NRF52832 BLE SOC-Nordic Semiconductor—Fig. S6) with a commercially available potentiostat chip

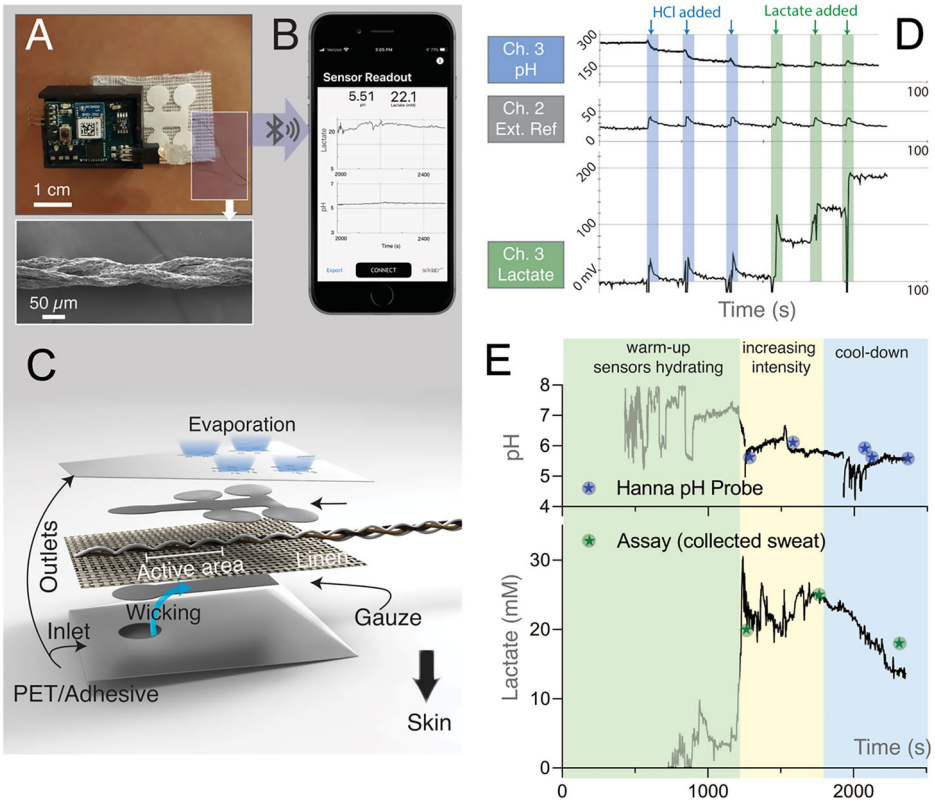

Fig. 4 | Device prototype. A On body testing setup including readout electronics, sensor braid and encapsulation patch. **B** Screen capture of iOS application with real-time readout of pH and lactate sensor values. **C** Exploded diagram of multi-layer encapsulation patch for on-body testing. **D** Verification of mobile readout electronics with benchtop testing showing simultaneous outputs from pH and lactate sensors, and an external reference electrode (Ag/AgCl). NaOH (~0.4 pH change) and lactate (1 mM) were added showing raw output (in mV) with no observable crosstalk aside from stirring-induced noise. **E** On body testing data from participant 1 collected during stationary biking. Simultaneous readout of pH and lactate data from the sensor patch correlated with a skin pH probe (Hanna) and L-lactate assay kit (recorded downstream from collected sweat at multiple time points).

(LMP91000, Texas Instruments). A custom-written iOS app is used for data collection from the interface.

An evaluation of crosstalk between channels of the system is presented in Fig. 4D. For this test, a pH sensor (Ch1), lactate sensor (Ch3), reference electrode, and external double junction reference electrode (Ch2) were connected to the readout PCB. Sequential additions of HCl and lactate to the beaker demonstrate that the current and potential measurements are decoupled, aside from stirring-induced noise.

On-body testing of demonstrator device

Testing of the sensor patch is performed on two human subjects during exercise on a stationary bike. The output is validated against a commercial pH meter (Hanna) and with chemically assayed sweat samples collected at multiple time points (tested using the Sigma MAK329 for lactate evaluation). The patch is adhered to the lower back of the participant, then the socket interface is connected to the readout integrated front-end. The latter is adhered over the patch during testing as shown in Fig. 4A. Data from the sensor is collected during a 30 min cycling workout using the custom iOS application (Fig. 4B). A comparison of the data obtained from the yarn with commercial measurements shows high correlation as well as good agreement with expected exercise-induced trends[1,6].

Simultaneous pH and lactate data from male participant 1 are shown in Fig. 4E. After 10 min, the sensing configuration begins to hydrate, with both lactate and pH sensors fully hydrated after 20 min. Improvements in integration/patch design and material selection can decrease this hydration time but were not the focus of this study. The data from the lactate sensor follows a typical sweating pattern with increasing lactate during high-intensity exercise, followed by a slow decline in lactate during the cool-down period. The pH sensor shows a value of pH 5.5–6, which requires a baseline correction of +40% for the lactate sensor. Temperature in the patch, measured in a separate cycling test (via a thermocouple placed in the patch), is 29–30 °C after sweating begins. A calibration correction of −15% accounts for this temperature difference. Following pH/temp baseline corrections, the lactate data is found to correlate well to the downstream analysis (via commercially available kit) on collected sweat. Data from female participant 2 is shown in Fig. S7. Similar high correlation between sensor and probe/assay is found. In this case, the pH values detected are near 7.9, and no corrections were required aside from temperature. Sex, skin-care products, measurement site, and sweat rate are some examples of parameters that affect sweat pH, highlighting the importance of inclusion of calibration elements in the yarn to allow for simultaneous pH sensing and correction of the measured physiological parameters[60].

Conclusions

rGO-based fibers are a promising material platform for embedded textile biosensor electrodes due to the inherent electrical, mechanical, and electrochemical properties of graphene, ease of fabrication, tunability of the fibers, and inexpensive material cost. Applications for these fibers range from low-cost disposable chemical sensors to wearable energy storage to lightweight interconnects. In the electrochemical yarn configuration demonstrated here, nanomaterial functionalization of these fibers enables simultaneous pH and lactate sensing in a convenient textile-ready format.

Solution-based processing allows for facile coating of large lengths of fiber with platinum nanoparticles, with stable performance as a mediator for H_2O_2. Further coatings with Nafion, biopolymer-embedded LOx, and a spray-coated diffusion layer of PU enable sensing of lactate in sweat with extended linear range. Real-time sweat sensing from a pH/lactate fiber bundle with high correlation to external measurements demonstrates the potential of these fibers in a wearable electrochemical sensing configuration. Further functionalization with various 1D and 2D nanomaterials and coatings with active membranes will enable a platform of textile-integrated electrochemical yarns of broad utility and use.

Methods

rGO fiber synthesis

GO dope (in 50% ethanol, 10 mg mL^{-1}) was dry-spun using a custom dry-spinning setup at a rate of 2–5 mm s^{-1} using 100 or 200 μm diameter needles. Fiber spools were reduced using a solution of hydriodic acid and

ethanol in a 1:4 ratio at 80 °C for 4 h. The spools were rinsed in ethanol three times, dried at 60 °C, then stored at room temperature.

Electroless deposition of platinum nanoparticles on rGO fiber

Hexachloroplatinic acid was added to ethylene glycol to a concentration of 10 mM. A 4:1 molar ratio of sodium hydroxide to platinum salt was formed by adding 1 M NaOH in ethylene glycol to the solution until a concentration of 40 mM was reached. A length of rGO fiber was either treated with one pass of a corona wand (Electro-Technic, BD-20AC) or oxygen reactive ion etch (Diener Zepto, 30 s, 50 W), loosely spooled, then was added to the solution. The speed of the corona wand process was preferred. After 30 min of soaking, the solution was heated in an oil bath at 110–115 °C for 2 h, until the solution turns from orange to brown to black. The spool was removed, allowed to cool to room temperature, and then rinsed with ethanol three times. The spool was dried at room temperature overnight.

Lactate sensor fabrication

A 1% solution of chitosan was prepared in 1% acetic acid, then adjusted to pH 5.5 with 1 M NaOH. Silk fibroin (30 min boiling) was prepared from Bombyx Mori cocoons according to established protocols[61,62]. The chitosan and silk fibroin solutions were stored at 4 °C until used. LOx (100 U) was combined with 25 µL silk fibroin (1.0% w/v), 250 µL DI water, 250 µL chitosan (1.0% w/v), and 22 µL 1% glutaraldehyde (0.08 M final concentration). The solution was thoroughly mixed and left at room temperature for 20 min. For full-length sensor fibers, 10 cm of PtNP-rGO was cut, then 1.5 cm of the fiber was dip-coated in 1% Nafion (diluted with 1x PBS), then dried at 60 °C. The fiber was then dip-coated in the enzyme mixture, forming a thick coating (5–10 µm) over the Nafion. The layer was dried for 1 h at room temperature, then the membrane was sprayed with 0.25% PU in THF forming the diffusion-limiting layer. The remainder of the sensor was sprayed with 1% PU in THF. The sensors were stored dry at 4 °C until use, up to 2 weeks.

Sensor characterization

SEM images of PtNP-rGO and enzymatic membrane were acquired using a Zeiss EVO SEM with 10 kV acceleration voltage. Benchtop electrochemical measurements of PtNP-rGO and lactate sensors were performed using an electrochemical workstation (Biologic SP-150) in a three-electrode configuration using a platinum wire counter electrode and a double junction Ag/AgCl reference electrode (Sigma 16811). Sections of PtNP-rGO (15 mm lengths, unless specified) were cut and fixed to crimp pins with silver paste, then the connection was isolated with hot-melt adhesive. CV of PtNP-rGO (scan rate, 50 mV s^{-1}) was performed in 0.5 M H_2SO_4 with a salt bridge (100 mM $NaSO_4$) to prevent chloride contamination from the reference. H_2O_2 sensitivity tests (CV, 50 mV s^{-1}, and CA, 0.5 V vs Ag/AgCl) were performed in 100 mM NaCl and 10 mM phosphate buffer. EIS was performed on rGO and PtNP-rGO in 5 mM potassium ferricyanide/ferrocyanide with an ionic background of 100 mM KCl.

Lactate sensors were first characterized with CA (0.5 V vs. Ag/AgCl) in 10 mM phosphate buffer (pH 7.4) with 5 mM additions of lactate. Interference tests were performed in 10 mM phosphate buffer with additions of 5 mM lactate, 10 mM Na^+, 1 mM Mg^{2+}, 1 mM Ca^{2+}, 1 mM glucose, and 100 µM ascorbic acid. pH sensitivity was measured in 10 mM phosphate-citrate buffer and 10 mM lactate with the pH adjusted between 5.5 and 8 using 1 M HCl and 1 M NaOH. Temperature sensitivity was measured with the electrochemical cell on a hotplate at 50 °C with stirring. The temperature of the solution and current from the sensor in 10 mM lactate and 10 mM phosphate buffer were measured concurrently.

On body testing

The validation and evaluation of the sensing bundle were performed with human subjects in compliance with a protocol (ID 19-04032) that was approved by the institutional review board at Tufts University. All subjects gave written, informed consent before participating in the study.

10 cm lengths of the counter electrode (PtNP-rGO), reference electrode, pH sensor, and lactate sensor were connected to a 6-pin socket, then braided together (additional details on the yarn assembly and braiding are described in ref. 27). The sensor bundles were calibrated in artificial sweat solutions with 2-point calibrations for pH (5, 7) and lactate (0, 20 mM). The bundle was woven into a piece of linen fabric, then sandwiched between laser-patterned gauze, filter paper, and double-sided adhesive PET films. The patch was adhered to the lower back, then the readout PCB (in a 3D-printed holder) was connected and adhered to the top surface. While the participant cycled on a stationary bike, pH measurements were taken with a skin pH probe (Hanna Instruments, HI99181) to evaluate correlations between the analytical standard (pH probe) and the sensing device here presented. The commercial pH meter was placed near the sensor patch, and readings were taken twice on average during the following: (1) active biking (i.e., "increasing activity" time span): 20 and 25 min after the start of the biking session; (2) "cool down" time frame: 3 and 5 min after the end of the biking session, which lasted an average of 30 min. Additionally, sweat was collected with filter paper encapsulated by Tegaderm at a location near the sensor patch. The patch was removed, immediately sealed, and replaced twice during biking and once at the end of the "cool down" period. Lactate levels were measured on average during the following time spans: (1) active biking (i.e., "increasing activity" time span): 20 and 25/30 min after the start of the exercise session (the latter usually being the end of the session); (2) "cool down" time frame: 5 min after the end of the biking session, which lasted an average of 30 min. The filter paper was centrifuged at 10,000 *g*, then the collected sweat was diluted down to 8× and 16× and assayed using a colorimetric lactate assay (Sigma MAK329) according to the kit's SOP.

Readout electronics

A custom small form factor 4-layer PCB (1.5 × 2 cm) was developed incorporating a Nordic NRF52832 BLE SOC, a Texas instruments LMP91000 potentiostat, a dual high input impedance operation amplifier (>1 TΩ) and supporting circuitry. The PCB was designed with minimal components, size (limited to the size of the smallest coin cell battery available (CR1216)), and power consumption. During operation it has a low average current draw of 140 µA, allowing for 5 days of continuous measurement with 2 small CR1216 batteries. The output of the LMP91000 (lactate) and voltage buffer (potentiometric) was fed to the analog inputs of the SOC (12-bit SAADC). The sample rate for each channel was 3 Hz with 8× oversampling for noise reduction. Data was post-processed using a moving average filter with a 15-point window.

Data availability

The main data that support the findings of this study are available in this article and its Supplementary Information. Any other relevant data are available from the corresponding authors upon reasonable request.

Received: 15 April 2023; Accepted: 18 October 2024;
Published online: 08 November 2024

References

1. Gao, W. et al. Fully integrated wearable sensor arrays for multiplexed in situ perspiration analysis. *Nature* **529**, 509–514 (2016).
2. Oh, S. Y. et al. Stretchable conductive composites integrated with soft electronics for strain/pressure sensors. *ACS Appl. Mater. Interfaces* **10**, 13729–13737 (2018).
3. Huang, X. et al. Stretchable, wireless sensors and body area networks for continuous bio-monitoring of physiological and mental well-being. *Small* **10**, 1–12 (2014).
4. Guinovart, T. et al. A potentiometric tattoo sensor for monitoring ammonium in sweat. *Analyst* **138**, 7031–7038 (2013).
5. He, W. et al. Integrated textile sensor patch for real-time and continuous sweat monitoring. *Sci. Adv.* **5**, eaax0649 (2019).
6. Anastasova, S. et al. A wearable multisensing patch for continuous sweat monitoring. *Biosens. Bioelectron.* **93**, 139–145 (2017).

7. Bandodkar, A. J., Jeerapan, I. & Wang, J. Sweat-activated electrochemical sensors for on-body monitoring. *ACS Sens.* https://doi.org/10.1021/acssensors.6b00250.
8. Yu, Y. et al. A soft sensor integrated wearable system for sweat biomonitoring during exercise. *Sci. Robot.* **5**, e7946 (2020).
9. Seshadri, D. R. et al. Wearable sensors for integrated health monitoring and sports performance analytics. *npj Digit. Med.* **2**, 1–14 (2019).
10. Parlak, O. et al. Flexible and stretchable electronic skin interfaces for digital health. *Sci. Adv.* **4**, eaar2904 (2018).
11. Wang, L. et al. Wearable artificial nerve enabled by smart textile electronics. *Adv. Funct. Mater.* **28**, 1804456 (2018).
12. Terse-Thakoor, T. et al. Smart headwear for cognitive monitoring. *npj Flex. Electron.* **4**, 1–8 (2020).
13. Wang, R. et al. Stretchable, ultra-thin epidermal strain sensors. *J. Mater. Chem. B* **8**, 3655–3664 (2020).
14. Lee, J. et al. A wearable multimodal sensor for health monitoring. *Adv. Mater.* **32**, https://doi.org/10.1002/adma.201902532 (2020).
15. Fang, B. et al. Nanomaterials for flexible and stretchable electronics. *Adv. Mater.* **32**, 1902664 (2020).
16. Eom, W. et al. A wearable biosensor for continuous sweat monitoring. *Nat. Commun.* **11**, https://doi.org/10.1038/s41467-020-16671-1 (2020).
17. Dreyer, D. R., Park, S., Bielawski, C. W. & Ruoff, R. S. The chemistry of graphene oxide. *Chem. Soc. Rev.* **39**, 228–240 (2010).
18. Jalili, R. et al. Organic/inorganic hybrid stretchable conductors. *Adv. Funct. Mater.* **23**, 5345–5353 (2013).
19. Lee, S. H. et al. Self-powered wearable sensor for environmental monitoring. *ACS Appl. Mater. Interfaces* **12**, 10434–10444 (2020).
20. Trung, T. Q. et al. Stretchable, transparent electronic skin with multifunctional sensing capabilities. *Adv. Healthc. Mater.* **7**, https://doi.org/10.1002/adhm.201800074 (2018).
21. Peng, Y. et al. Flexible hybrid nanocomposites for energy conversion applications. *Carbon* **136**, 329–339 (2018).
22. Yeo, C. S. et al. Smart textile-based wearable systems for health monitoring. *J. Mater. Chem. C* **5**, 12825–12835 (2017).
23. Tian, Q. et al. Multiscale assembly of functional nanomaterials for high-performance energy storage. *Nanoscale* **9**, 12335–12346 (2017).
24. Li, P. et al. Flexible and stretchable piezoelectric nanogenerators for energy harvesting. *Adv. Funct. Mater.* **30**, https://doi.org/10.1002/adfm.202006584 (2020).
25. Fan, L. et al. Graphene-based materials for flexible supercapacitors. *J. Mater. Chem.* **22**, 6165–6173 (2012).
26. Jayaramulu, K. et al. Covalent Graphene-MOF Hybrids for High-Performance Asymmetric Supercapacitors *Adv. Mater.* **33**, 2004560 (2020).
27. Napier, B. S., Matzeu, G., Lo Presti, M. & Omenetto, F. G. Silk-based wearable devices for healthcare. *Adv. Mater. Technol.* **7**, https://doi.org/10.1002/admt.202101508 (2022).
28. Yang, Q. et al. Multifunctional flexible hybrid energy storage systems. *J. Mater. Chem. A* **5**, https://doi.org/10.1039/c7ta07999k (2017).
29. Zhou, T. et al. Bioinspired flexible materials for mechanical energy harvesting. *Nat. Commun.* **11**, https://doi.org/10.1038/s41467-020-15991-6 (2020).
30. Li, Y. et al. Conductive nanocomposites for stretchable electronics. *NPG Asia Mater.* **7**, https://doi.org/10.1038/am.2014.111 (2015).
31. Hua, L. et al. Flexible electronic skins with integrated tactile sensing. *ACS Appl. Mater. Interfaces* **9**, 37022–37030 (2017).
32. Chen, D., Feng, H. & Li, J. Graphene-based materials for electrochemical sensors. *Chem. Rev.* **112**, 6027–6053 (2012).
33. Zhou, M., Zhai, Y. & Dong, S. Recent advances in graphene-based electrochemical biosensors. *Anal. Chem.* **81**, 5603–5613 (2009).
34. Vaidya, R., Atanasov, P. & Wilkins, E. Biosensor-based monitoring systems. *Med. Eng. Phys.* **17**, 416–423 (1995).
35. Abrar, M. A., Dong, Y., Lee, P. K. & Kim, W. S. Graphene-based smart textiles for wearable biosensors. *Sci. Rep.* **6**, 1–9 (2016).
36. Zhao, Y. et al. Graphene-based wearable sweat sensors for continuous monitoring. *Sci. Adv.* **6**, eaaz0007 (2020).
37. Rocchitta, G. et al. A portable electrochemical biosensor for in situ monitoring of lactate. *Sensors* **16**, 780 (2016).
38. Wang, Y. et al. Multifunctional graphene-based wearable textiles. *Mater. Today* **21**, 186–194 (2018).
39. Noh, S. H. et al. Flexible, stretchable electronics for wearable healthcare applications. *Carbon* **142**, 230–238 (2019).
40. Xin, G. et al. High-performance wearable thermoelectric generators. *Science* **349**, 1083–1087 (2015).
41. Oh, H. S., Oh, J. G., Hong, Y. G. & Kim, H. Electrochemical performance of Pt-free cathodes in PEMFCs. *Electrochim. Acta* **52**, 7278–7285 (2007).
42. Konkena, B. & Vasudevan, S. Electrochemical analysis of graphene-based materials. *J. Phys. Chem. Lett.* **3**, 13–20 (2012).
43. Variava, M. F., Church, T. L., Harris, A. T. & Minett, A. I. MOF-derived graphene composites for energy applications. *J. Mater. Chem. A* **1**, 8509–8520 (2013).
44. Li, Y. et al. Wearable graphene-based strain sensors for human motion monitoring. *Carbon* **48**, 1124–1130 (2010).
45. Hoe, L. P., Boaventura, M. & Lagarteira, T. Hydrogen production using metal-organic frameworks. *Int. J. Hydrog. Energy* **43**, 16998–17005 (2018).
46. Lagarteira, T. et al. Metal-organic frameworks for efficient hydrogen storage. *Int. J. Hydrogen Energy* **45**, 20594–20602 (2020).
47. Steinfeldt, N. Bioinspired self-cleaning surfaces. *Langmuir* **28**, 13072–13079 (2012).
48. Kondratowicz, I. et al. Conductive polymers for energy storage. *Appl. Surf. Sci.* **440**, 651–659 (2018).
49. Lee, K. et al. Wearable strain sensors using graphene-based materials. *Sci. Rep.* **9**, 1–9 (2019).
50. Lu, J., Li, Y., Li, S. & Jiang, S. P. High-performance oxygen evolution catalysts. *Sci. Rep.* **6**, 1–10 (2016).
51. Halder, A., Sharma, S., Hegde, M. S. & Ravishankar, N. Nanostructured oxides for electrochemical applications. *J. Phys. Chem. C* **113**, 1466–1474 (2009).
52. Doña Rodríguez, J. M., Melián, J. A. H. & Peña, J. P. Photocatalytic oxidation of organic pollutants. *J. Chem. Educ.* **77**, 1195–1200 (2000).
53. Payne, M. E. et al. Skin-conformal, wearable electronic systems for human motion detection. *Sci. Rep.* **9**, 13720 (2019).
54. You, Y. et al. Soft, stretchable biosensors for continuous sweat monitoring. *Sci. Robot.* **5**, eaaz7946 (2020).
55. Jia, W. et al. Electrochemical tattoo biosensors for real-time analysis. *Anal. Chem.* **85**, 6553–6560 (2013).
56. Hu, Y., Zhang, Y. & Wilson, G. S. Electrochemical glucose sensors. *Anal. Chim. Acta* **281**, 503–509 (1993).
57. Lewenstam, A., Blaz, T. & Migdalski, J. Ion-selective electrodes for clinical analysis. *Anal. Chem.* **89**, 1068–1075 (2017).
58. Mostafalu, P. et al. Wearable bioelectronics for personalized health monitoring. *Microsyst. Nanoeng.* **2**, 16039 (2016).
59. Bandodkar, A. J. et al. Soft, stretchable, and flexible wearable sensors for physiological monitoring. *Sci. Adv.* **5**, eaav3294 (2019).
60. Baker, L. B. Hydration assessment during exercise. *Temperature* **6**, 211–222 (2019).
61. Rockwood, D. et al. Materials based on silk proteins. *Nat. Protoc.* **6**, 1–13 (2011).
62. Guidetti, G. et al. Silk-based bioelectronics: materials and applications. *Appl. Phys. Rev.* **9**, 011302 (2022).

Acknowledgements

The authors acknowledge support from the Office of Naval Research (N00014-19-1-2399) for this work.

Author contributions

B.N., G.M., and F.G.O. conceived the idea. B.N., G.M., and F.G.O. designed the experiments. B.N. and G.M. performed the experiments. B.N. and G.M. analyzed the data. B.N., G.M., and F.G.O. reviewed the data and wrote the manuscript. F.G.O. supervised the activities.

Competing interests

Intellectual property based on the methods and approaches described in the paper has been filed by Tufts University.

Additional information

Supplementary information The online version contains supplementary material available at https://doi.org/10.1038/s43246-024-00680-4.

Correspondence and requests for materials should be addressed to Fiorenzo G. Omenetto.

Peer review information *Communications Materials* thanks the anonymous reviewers for their contribution to the peer review of this work. Primary Handling Editors: Rona Chandrawati and John Plummer.